7th International Conference & Exposition on Petroleum Geophysics

"HYDERABAD 2008"

P - 33

An Integrated Geophysical approach for Sub-Basalt Imaging: A Case Study, Jam River Basin, India

V. Chakravarthi

DRS Group, National Geophysical Research Institute, Uppal Road, Hyderabad – 500 007, India
vcvarthi@rediffmail.com

Summary

An integrated geophysical strategy comprising deep electrical resistivity and gravity data to image sub-basalt sedimentary basins is presented. A 3D gravity inversion is used to determine the basement structure of the Permian sediments underlying the Cretaceous formation of the Jam River Basin, India. The thickness of Cretaceous formation above the Permian sediments estimated from modeling of 60 deep electrical sounding data agree well with drilling. The gravity effect of mass deficit between the Cretaceous and Permian formations was found using a 3D forward modeling and subsequently removed from the Bouguer gravity anomaly along with the regional gravity field. The modified residual gravity field was then subjected to 3D inversion to map the variations in depth of the basement beneath the Permian sediments. Inversion of gravity data resulted two basement ridges, running almost E-W, dividing the basin into three independent depressions. It was found that the Katol and Kondhali faults were active even during the Post-Cretaceous time and were responsible for the development of the subsurface basement ridges in the basin. The inferred 3D basement configuration of the basin clearly brought out the listric nature of the two faults referred earlier. Further, the extension of the Godavari basin into the Deccan syneclise and the fact that the source rock studies show the presence of hydrocarbons in the Sironcha block in the northern part of the Godavari basin would throw some light on the hydrocarbon potential of the Jam River Basin as well.

Introduction

The discovery of commercial oil and gas fields besides the coal bed methane in the Gondwana sediments of Permo-Triassic age in Krishna-Godavari (KG) sub-basin, and the fact that the source rock studies show the presence of hydrocarbons in the Sironcha block in the northern part of the Godavari basin, India drew the attention of major oil industries to explore and ascertain the natural resources in and around the Jam River Basin (JRB), India as the Godavari basin extends further northwest across the Deccan Syneclise (Figure 1). Gondwana sediments of Permo- Triassic age are also present in JRB concealed under basalts (Figure 2) and at a few selected places on the eastern side exposed to the surface as linear patches (Murthy et al., 1986). The Gondwana sediments in turn rest unconformably over the Archaean basement. Although, a limited number of shallow boreholes were drilled in JRB (Chakraborti and Mungal, 1995), no exploratory well was drilled so far in the basin to greater depths to find the traces of oil and gas. Although Pant et al. (1983) have carried out geological and geophysical surveys in JRB, the structural configuration of the basement beneath the Permian sediments is yet to be delineated. On the other hand, Sarma

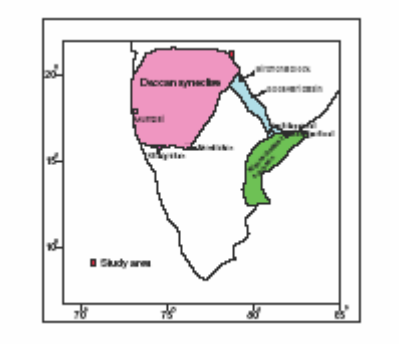

Figure 1: Location map of Godavari and jam River Basins, India.

et al. (2004) have conducted regional magnetotelluric (MT) surveys in the basin at random intervals along a few selected traverses and estimated the basement configuration based on 1D and 2D inversion of MT data, however, 3D configuration is yet to be realized. It can be stated in unequivocal terms that the spatial location of sub-basalt targets and geological translation of geophysical measurements/interpretation still poses a formidable challenge to the practicing geophysicists and at times continues to be cumbersome. Imaging of sub-basalt structures by conventional P-wave seismic survey is often problematic. In recent times, geophysical prospecting have moved towards the use of integration of potential fields and electrical methods for regional and prospect evaluation prior to drilling and such an integrated strategy has been proven cost effective for exploration in basalt-covered area (Prieto et al., 1985, Mitsuhata et al., 1999).

The geological purpose of the integrated study in this paper is to evaluate the 3D configuration of the basement structure of JRB from integrated modeling of Deep Electrical Sounding (DES) and gravity data and to investigate the possibilities of hydrocarbon prospectivity in the basin. This study may effectively find application in the exploration of hydrocarbons.

Geology

The geology of JRB and adjoining areas is shown in Figure 2. The topography of the basin is moderate in nature with the master slope being towards the north. The elevation of the topography varies between 200 to 400 m above mean sea level (Figure 3). The Jam River originates near Dhanoli village in the southern tip of the basin, flows northward up to Panchdhar and then takes a northwest trend up to Digras and finally flows in NNW before joins the Wardha river (Figure 3). The JRB is covered with flood basalt of the Cretaceous-Eocene age. In the southern part of the basin around Jatlapur, 10-12 m thick Laterite occurs as cap rock over the flood basalt (Figure 2). A thin layer of vesicular/ Amygdular basalt with a few meters in thickness forms the upper horizon of some of the basalt flows. Vesicular basalts are softer than massive basalts and vesicles are filled with secondary minerals like calcite, zeolites and quartz. Their exposures are seen at the centre of the basin, between Katol and Kondhali and also around Chikhli. On the other hand, massive basalts are compact, grayish black in color and show a fragmentary structure up to a depth of 1-2 m and mostly occupy 80 to 90 percent of the area. White friable limestone intertrappean exposures are seen southwest of Kondhali (Figure 2). Deshmukh et al. (1990) have reported two prominent faults within the basin, one near Katol and the other near Kondhali (Figure 2).

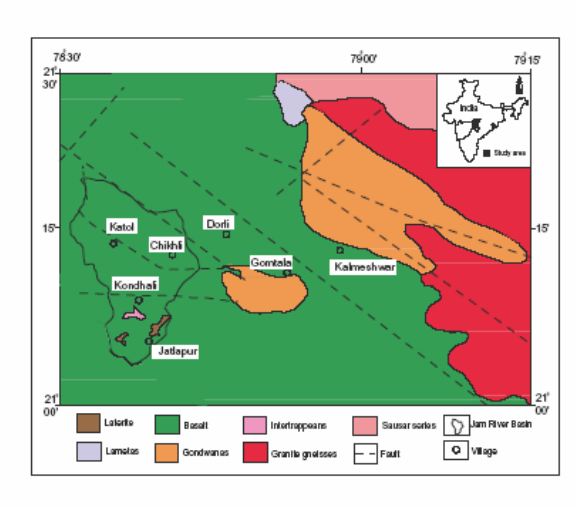

Figure 2: Geology of Jam River Basin and adjoining areas, India.

Based on the structural setting, the basin can be divided into 3 units (Figure 3) namely, i) the southern block (between Mendepathar and Dhanoli), ii) central block (between Mendepathar and Mendhepathar), and iii) the northern block (between Mendhepathar and the confluence of Jam River with Wardha River). The WNW-ESE strike of the exposed Gondwana sediments on the eastern side of the basin (Figure 2) suggests that these rocks are likely to extend beneath the basalt flows within the basin (Murthy et al., 1986).

Geophysical Surveys

Although, many 2D techniques to model basalt covered areas are available (Prieto et al., 1985, Ferguson et al., 1988), modeling by 3D schemes would be more appropriate because the strike lengths of many sedimentary basins are limited. Based on integrated modeling of deep resistivity and gravity data, we bring out here a clear picture of the 3D basement configuration of the Jam river basin, India.

In this direction, as many as 60 DES with a maximum current electrode separation ranging from 1.5-2.0 km using the Schlumberger electrode configuration were conducted in the basin (Figure 3) to identify the basalt-sediment interface.

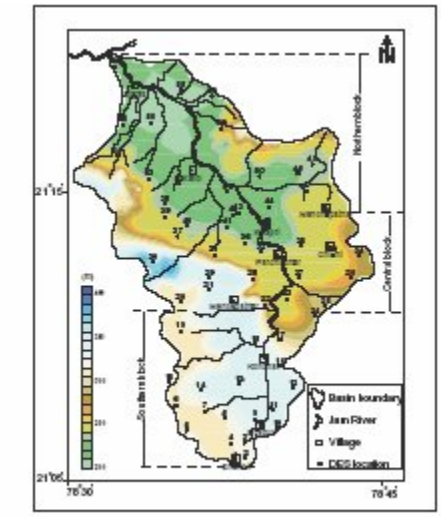

Figure 3: Topographic relief, drainage network and locations of DES stations, Jam River Basin, India.

At the middle of the basin in block 1, KHK type curves were noticed at 27 sounding stations. The descending nature of sounding curves (for eg., DES 37 and DES 35) at larger current electrode separation (Figure 4a) invariably show the presence of low resistive Gondwana sediments at depth. In south, between Mendepathar and Dhanoli (Figure 3), 19 soundings were conducted which exhibit ascending trend at larger current electrode separations (Figure 4b). It may be noted from Figures 4a and b that the behavior of sounding curves at larger electrode separation at the centre could not be seen in the southern block (DES 2 and DES 18), which in turn reveals that a current electrode separation of 2.0 km may be inadequate to get the signal due to sediments, if any. In the northern block (Figure 3), 14 soundings were conducted and some of the typical sounding curves (DES 48 and DES 56) are shown in Figure 4c. The sounding curves in Figure 4c show an increasing trend with the increase of current electrode separation and tend to attain a decreasing trend. All the sounding curves were interpreted in terms of geoelectrical parameters (Mukarami et al., 1986) and subsequently, two boreholes were drilled, one at Chikhli (DES-33) and the other at Katol (DES-52). At Chikhli, the borehole encountered the the Gondwana sediments at a depth of 119 m over a drilled depth of 150m, whereas, at Katol, no sediments were encountered up to a drilled depth of 264 m. The lithological

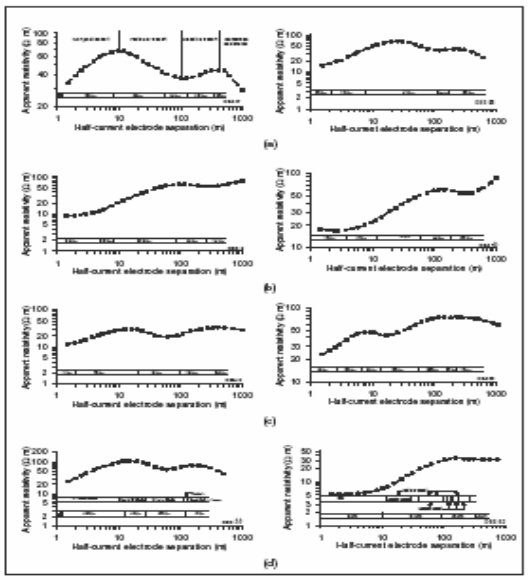

Figure 4: Observed (—) and modeled (•••) sounding curves, DES 37 and DES 35 in central block (a), DES 2 and DES 18 in southern block (b), DES 48 and DES 56 in northern block (c), and DES 33 and DES 52 at Chikhli and Katol along with lithological logs (d)

sequences, the observed and modeled sounding curves (DES 33 and DES 52) are shown in Figure 4d. The sounding curve at Chikhli (Figure 4d) clearly shows the presence of sediments beneath the basalt; however, at Katol it is not repeated.

The interpreted true resistivity of massive basalt is in the range of 150-450 Ω m, whereas for vesicular basalt it is 45 Ω m. At Katol, the resistivity of vesicular and massive basalts together is 55 Ω m. The significant resistivity contrast between the basalt (150-450 Ω m) and the underlying sediments (< 20 Ω m) may be attributed to the success of electrical method to delineate the concealed sediments beneath the basalt cover. The resistivities of formations inferred from test soundings (DES 33 and DES 52) are used to constrain the interpretation of other sounding data in the region. The modeled sounding curves in central, southern and northern blocks are shown in Figures 4a, b and c respectively. The thickness of basalt estimated from the interpretation of 60 DES data was then used to prepare an isopach contour map (Figure 5a). The thickness of basalt is found to be more than 0.35 km in northern and southern parts of the basin. By and large, the thickness of the basalt decreases from both north and south towards the center of the basin. It is also evident from Figure 5a that the sharp gradient in thickness of basalt between DES 32 and DES 27, and DES 42 and DES 44 at the centre (Figures 3 and 5a) may indicate a fault along which the Jam River apparently flows from south to north.

In short, the thickness of basalt estimated from the interpretation of DES compares well with the borehole information in and around the basin.

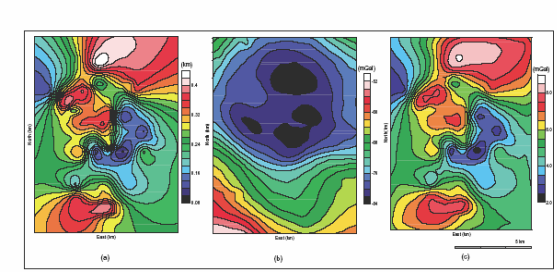

Figure 5: Isopach map of basalt (a), Bouguer gravity anomaly (b), and computed gravity effect of the mass deficit between the basalt and underlying sediments (c), Jam River Basin, India.

All gravity corrections including isostatic correction have been applied to the raw gravity data of the basin and the resulted Bouguer gravity anomaly reduced to the mean sea level was shown in Figure 5b (Murthy et al., 1986). A preliminary examination of the gravity data indicates that it could provide useful information on the structure of the basin. In spite of the fact that the gravity anomaly is very sensitive to near surface high density basalt, a large negative gravity anomaly in the basin (-80 mGal) suggests that the thickness of concealed sediments is of some significance. The steep gradient in the anomaly to the south of circular gravity low (Figure 5b) support the interpretation that this area is faulted and is of quite complex in nature. The Kondhali fault, which was mapped based on geological studies, coincides with this steep gradient. Further, the nosing of anomaly along NNW-SSE in the southern part of the basin could suggest yet another fault in the basement (Murthy, 1998, Chakravarthi and Sundararajan, 2004). The dislocation of -82 m Gal along a NW-SE trend at the centre of the basin is due to the Katol fault. The thickness of basalt varies quite significantly within the area (Figure 5a), and therefore, its gravity effect also varies accordingly. Thus, further processing of Bouguer gravity anomaly of the area is necessary prior to quantitative interpretation.

In the present study, the regional gravity field was determined by setting the areas of outcropping basement on the eastern side beyond the area of measurement to be equivalent to zero mGal. According to Abdoh et al. (1990), to determine the geometry of the base of Permian sediments, the gravity effect of the mass deficit between the basalt and the underlying sediments must be calculated and removed from the Bouguer gravity anomaly along with the regional gravity field. Removing the gravity effect of the mass deficit between basalt and sediments is tantamount to replacing the high-density overburden basalt by a fictitious homogeneous layer with a density akin to that of the underlying sediments. The measured average densities of basalt, Gondwana sediments and Granite gneisses are given as 2.85 gm/cm^3, 2.2 gm/cm^3 and 2.7gm/cm^3 respectively. A rectangular grid with as many as 660 grid nodes, 22 along the east and 30 along the north was used to approximate the isopach contour map of the basalt (Figure 5a). The grid nodes are selected at an interval of 1.25 km along both east and north. The gravity effect of the mass deficit between the basalt and sediments was then calculated with a density contrast of 0.65 gm/cm^3 using a 3D forward modeling code (Chakravarthi et al., 2002), GRAV3DBASE (code is available at http://www. iamg. org/CGEditor/ index. htm). The computed gravity effect is shown in Figure 5c. A maximum of an anomalous field of more than 8.5 mGal is observed in northern and southern blocks (Figure 5c) where the thickness of basalt attains its maximum (Figure 5a).

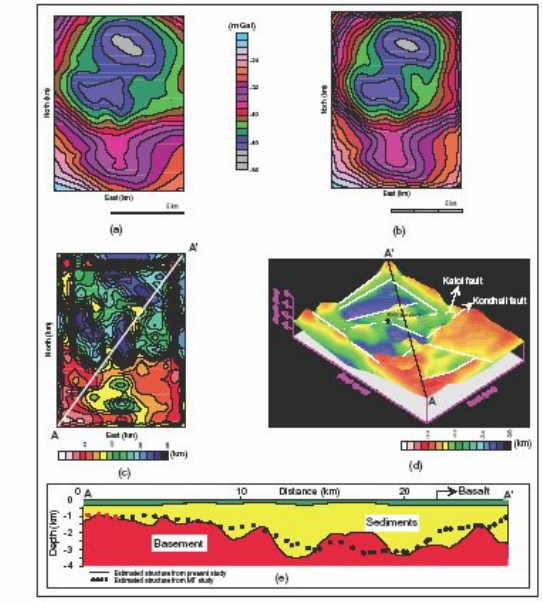

Figure 6: Modified residual gravity anomaly (a), modeled gravity anomaly subsequent to inversion (b), plan view of the basement structure (c), 3D view of the basement structure (d), and estimated depth from gravity and MT along the profile AA' (e), Jam River Basin, India.

Removal of the regional gravity field and the gravity effect of the mass deficit between the basalt and sediments (Figure 6c) from the Bouguer anomaly (Figure 5b) has resulted the modified residual gravity field (Figure 6a). It may be observed from the Bouguer (Figure 5b) and modified residual gravity (Figure 6a) fields that i) the circular gravity low observed in the Bouguer anomaly tend to be elliptical in the modified residual field with major axis of the anomaly striking along NE-SW, ii) trends of gravity lows within the circular anomaly become more pronounced along NW-SE, iii) the nosing of the anomaly along NNW-SSE in the Bouguer anomaly becomes more

prominent in the modified residual gravity field, and iv) the significant nosing along ENE-WSW in southwest of the basin, which was obscured in the Bouguer anomaly is clearly seen in the modified residual field.

For quantitative interpretation, the modified residual gravity field of the basin shown in Figure 6a was digitized into 660 grid nodes and inverted using a 3D inversion (Chakravarthi, 2003). The initial depths at all grid nodes were calculated based on the infinite slab formula and subsequently improved making use of Marquardt (1963) algorithm (Chakravarthi, 2003). A constant density of -0.5 gm/cm^3 between the sediments and basement was used in the inversion, as no density log was available to simulate the variation of density of sedimentary rocks.

The modeled gravity anomaly subsequent to inversion is shown in Figure 6b, whereas the inferred basement structure in plan and 3D views are shown in Figures 6c and d respectively. By and large, the modeled gravity anomaly shown in Figure 6b compares well with the observed one (Figure 6a). It can be seen from Figures 6c and 6d that the basement deepens towards the north. The Katol and Kondhali faults (Figure 2), which were mapped based on geological studies (Deshmukh et al., 1990), were clearly brought out in the inferred structural model too (Figure 6c and d). A trough like depression can be seen in the middle of the basin. Two conspicuous basement ridges run almost E-W divide the basin into three independent depressions (Figures 6c and d). The subsurface basement ridge in the northern block is controlled by the Katol fault towards the south.

Figure 6e shows the depth section of the inferred basement from gravity inversion along the profile AA'. The basalt-sediment interface is also plotted along the same profile. It can be seen that the thickness of basalt almost remains the same on either ends of the profile except at the centre over the basement ridges. This would mean that the basement might have been uplifted subsequent to the deposition of the sediments and basalt along the preexisting Katol and Kondhali faults consequently affecting the thickness of these two. The convex nature of the base of basalt over the subsurface ridges is a testimony to such uplift (Figure 6e). Further, a borehole (shown as PKV in Figure 6d), which was drilled to the south of the basement ridge, has encountered artesian conditions and yields ground water continuously. It is to be noted from Figure 6d that the basement ridge may act as a subsurface barrier to the ground water flow, and the Katol fault (Figure 6d) behaves as a conduit to the movement of ground water, and hence artesian conditions are developed in the region. The 3D basement configuration of the basin also brought out well the listric nature of the Katol and Kondhali faults (Figure 6d).

The basement configuration derived from MT along the same gravity profile, AA', (Sarma et al., 2004) is also shown in Figure 6e for comparison. By and large, the depth sections derived from both gravity and MT compare well with each other with a couple of exceptions. For eg., i) the width of the basement ridge derived from MT in NE-SW (Figure 6e) at the centre of the basin is much smaller than the corresponding one estimated from gravity, and ii) the basement structure derived from MT shows an up warp in the northeastern part (Figure 6e) whereas it is not so in the case of gravity. In the present case, the dimensions of the basement ridge derived from gravity may be more reliable because the gravity anomaly over the ridge shows significant wavelength (Figure 6a). So also, the continuation of gravity low over and beyond the boundary of the basin in the north, the NW-SE trending major fault in the northern boundary (Figure 2), and the NW-SE strike of the exposed Gondwana sediments in northeastern part beyond the boundary of the basin near Kalmeshwar (Figure 2) supports the gravity interpretation that the basement may deepen further north (Figure 6e). It is also to be noted that unlike in the case of gravity, the MT cross-section was prepared by interpolation of depth among randomly spaced stations (Sarma et al., 2004) along the profile, AA', and, hence some features might not be delineated properly. On the other hand, the model estimated from 3D gravity inversion supported by DES data yields a geologically plausible model of the basin.

The maximum depth to the basement at the centre and in northern blocks is in excess of 3.2 km. The thickness of sediments in Sironcha block in the northern part of the Godavari basin (Figure 1) is about 4.0 km (Agarwal, 1995) and compares well with the estimated thickness of sediments in JRB. Further, the source rock studies using comprehensive modern techniques of the organic rich samples of carbonaceous shales and coal in Mandapeta and Aswaraopet wells as well as Sironcha block (Figure 1)

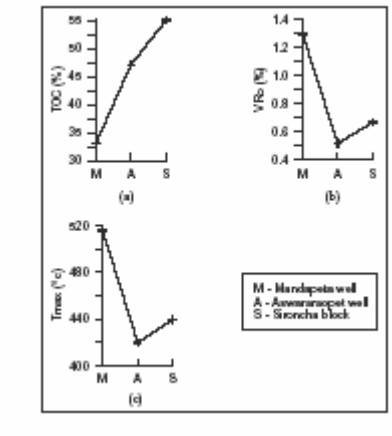

Figure 7: Measured TOC (a), VRo (b), and Tmax (c) at Mandapeta well, Aswaraopet well and Sironcha block, Godavari basin (after Prabhu et al., 1992; Samanta et al., 1993; Agarwal, 1995).

show significant quantities of total organic carbon (TOC), vitrinite reflectance (VRO) and thermal exposure (Tmax) (Prabhu et al., 1992; Samanta et al., 1993; Agarwal, 1995). Figure 7 shows a comparison of the measured TOC, VRO, and Tmax at Mandapetta and Aswaraopet wells and Sironcha block. It can be seen from Figure 7a that the measured TOC in Sironcha block shows much higher value than the corresponding ones measured at Mandapeta and Aswaraopet wells. The measured VRO (Figure 7b) and Tmax (Figure 7c) in Sironcha block also show higher values in comparison to the Aswaraopet well. Based on the geological and geochemical studies Agarwal (1995) showed that the Sironcha block is a potential zone for further exploration of hydrocarbons which in turn may also throw some light on the hydrocarbon potential of the JRB as well.

Conclusions

An integrated geophysical modeling employing deep resistivity and gravity data to decipher the basement configuration of sub-trappean sediments is suggested. A 3D configuration of the base of Permian sediments concealed under Cretaceous formation of the Jam River Basin, India was inferred from integrated modeling of deep resistivity and gravity data. The base of Cretaceous formation was estimated from modeling of 60 deep resistivity sounding data supported by drilling. The gravity effect of the deficit in mass between Cretaceous and Permian formations was computed in the space domain and then subtracted from the Bouguer gravity anomaly along with the regional field. A 3D inversion of the modified residual gravity resulted a maximum depth to the basement in excess of 3.2 km in central and northern parts. The faults which were mapped based on geological studies are brought out well from gravity modeling. The Katol and Kondhali faults were active during the Post-Cretaceous time also and might have been responsible for the development of subsurface basement ridges. It is observed that a basement ridge acting as a subsurface barrier to the flow of ground water is responsible for the development of artesian conditions at the centre of the basin. By and large, the cross-section of the estimated structure from gravity along SW-NE profile compares well with the structural model derived from MT. The estimated thickness of sediments in Sironcha block in the northern part of the Godavari basin compares well with the estimated thickness of the sediments in JRB. Since the Godavari basin extends further northwest into Deccan syneclise and also the fact that the source rock studies of the Sironcha block indicate good source rock potential capable of generating hydrocarbons this study would effectively find application in the exploration of hydrocarbons in JRB.

References

Agarwal, B. P., 1995, Hydrocarbon prospects of the Pranhita-Godavari graben, India: Proceedings of Petrotech, **95**, 115–121.

Abdoh, A., D. Cowan, and M. Pilkington, 1990, 3D gravity inversion of the Cheshire Basin: Geophysical Prospecting, **38**, 999-101.

Chakraborti, R. K., V. V. Mungal, 1995, Regional exploration by scout drilling for coal in and around Katol area, Nagpur district, Maharashtra: Records of Geological Society of India, **128**, 239-240.

Chakravarthi, V., H. M. Raghuram, and S. B. Singh, 2002, 3D forward gravity modeling of density interfaces above which the density contrast varies continuously with depth: Computers & Geosciences, **28**, 53-57.

Chakravarthi, V., 2003, Digitally implemented method for automatic optimization of gravity fields obtained from three-dimensional density interfaces using depth dependent density: US Patent 6 615 139.

Chakravarthi, V., and N. Sundararajan, 2004, Ridge regression algorithm for gravity inversion of fault structures with variable density: Geophysics, **69**, 1394-1404.

Deshmukh, S. S, S. M. Godbole, S. Balakrishnan, and A. K. Chatterjee, 1990, Compilation, synthesis and evaluation of available information on all aspects of Deccan Traps: Records of the Geological Survey of India, **123**, 210-233.

Ferguson, J. F., R. N. Flech, C. L. V. Aiken, J. S. Oldow and H. Dockery, 1988, Models of the Bouguer gravity and geologic structure at Yucca Flat, Nevada: Geophysics, **53**, 231-244.

Marquardt, D. W., 1963, An algorithm for least squares estimation of nonlinear parameters: SIAM Journal of Applied Mathematics, **11**, 431-441.

Mitsuhata, Y., K. Matsuo, and M. Minegishi, 1999, Magnetotelluric survey for exploration of a volcanic-rock reservoir in the Yurihara oil and gas field, Japan: Geophysical prospecting, **47**, 195-218.

Murakami, Y., A. Zerilli, and R. J. Bisdorf, 1986, A computer program for the automatic inversion of Schlumberger soundings using multi-layer interpretation followed by Dar Zarrouk reduction: Open File Report - U. S. Geological Survey.

Murthy, B. G. K., K. R. Rao, and D. V. Punekar, 1986, Report on the geophysical investigations for delineating Gondwanas below traps in Umrer, Bander, Kamthi and Katol troughs in Nagpur district: Deep Geology Project, Geological Survey of India, India.

Murthy, I. V. R., 1998, Gravity and magnetic interpretation in Exploration Geophysics: Memoir 40, Geological Survey of India, 1-363.

Pant, P. R., S. N. Lahiri, A. C. Khare, and R. C. Pathak, 1983, Seismics in exploration for coal – A case study in Kamptee coal field, Maharashtra: Special Publication Series - Geological Survey of India, **2**, 247-260.

Prabhu, B. N., K. B. Kohli, A. Mamgain, A. Pande, R. Dhawan and N. J. Thomas, 1992, Source rock potential of coals through hydrous anhydrous pyrolsis studies in Gondwana graben, Unpublished report of KDMIPE, Oil and Natural Gas Corporation, Dehradun, India.

Prieto, C., C. Perkins, and E. Berkman, 1985, Columbia River Basalt plateau, an integrated approach to interpretation of basalt-covered areas: Geophysics, **50**, 2709-2719.

Samanta, U., Misra, C. S., Jain, S., and Misra, K. N., 1993, Organic Geochemistry of Gondwana sediments in Pranhita-Godavari Grabens: Gondwana Geol. Magazine, Special Volume, Gondwana Geological Society, Nagpur, India, 349-361.

Sarma, S. V. S., T. Harinarayana, G. Virupakshi, M. Someswara Rao, Madhusudan Rao, Nandini Nagarajan, T. S. Sastry, and S. Prabhakar E. Rao, 2004, Magnetotelluric investigations in Deccan Trap covered areas of Nagpur-Wardha region, India: Journal of Geophysics, **25**, 87-91.

Acknowledgements

I am very much thankful to Dr. V. P. Dimri, Director, National Geophysical Research Institute, Hyderabad for his constant support and encouragement. The DRS data used in the present work was provided by Dr. D. Muralidharan of NGRI.